A Lattice-Boltzmann Based Method Applied to Digital Rock Characterization of Perforation Tunnel Damage

Bernd Crouse, David M Freed, Nils Koliha, Gana Balasubramanian EXA CORP
Rajani Satti, Derek Bale, Stephen Zuklic BAKER-HUGHES INC

This paper was prepared for presentation at the International Symposium of the Society of Core Analysts held in Snowmass, Colorado, USA, 21-26 August 2016

ABSTRACT

The lattice-Boltzmann method (LBM) for computational fluid dynamics has received considerable attention as a favorable approach for performing direct numerical simulation of pore-scale flow in porous media, especially for predicting permeability properties of reservoir rocks. The well recognized benefits of LBM as an approach for digital rock flow simulations include parallelizability, reliable convergence, and the opportunity to introduce multi-phase physics at the kinetic theory level. One of the challenges with LBM is to implement a surface boundary condition that avoids near-wall numerical issues, especially when portions of the relevant pore space are resolved with only a small number of grid cells. The present study examines LBM for digital rock using a boundary scheme based on explicit surface elements. A basic academic example of flow around packed spheres is presented, demonstrating the accuracy of the method even for coarse grid resolution. The method is then applied to the study of permeability alteration due to perforation tunnel damage. Using single-phase flow simulations based on micro-CT images of a small plug taken from a Berea sandstone test section, variations in porosity and absolute permeability of the damage zone around a typical perforation tunnel are characterized and visualized.

INTRODUCTION

Conceived about 30 years ago, the lattice-Boltzmann method (LBM) for computational fluid dynamics has become well established for various fluid flow applications [1]. An alternative to traditional Navier-Stokes PDE-based methods, LBM is based on kinetic theory and solves a discrete form of the Boltzmann transport equation for the fluid particle distribution function [2-5]. The usual implementation yields a flow simulator which is inherently transient, viscous, and uses a cubic lattice as the computational grid.

In addition to successful application to turbulent flow problems [6], LBM has recently received considerable attention as a favorable approach for performing direct numerical simulation (DNS) of pore-scale flow within porous media. A particularly active application area is digital rocks [7], in which fluid flow in petroleum reservoir rock samples is simulated in order to predict important petrophysical properties such as absolute permeability, relative permeability curves, and capillary pressure curves. In digital rocks, high resolution scanning is performed to obtain a 3D image differentiating the rock grains and pore space. Various image processing techniques are applied to

generate a sufficiently accurate representation of the pore space geometry to be suitable as input for analyses such as computational flow simulation [8].

There are well recognized benefits of LBM as an approach for such pore-scale flow simulation. The localized nature of the algorithm supports parallelization and scalability. The mesoscopic approach of tracking particle distributions provides a deep connection to the underlying statistical mechanics of fluid flow, giving rise to favorable accuracy, reliable solution convergence, and the opportunity to include complex physics (e.g. multi-phase flow [9]) in a more robust way than traditional Navier-Stokes methods. However, there are also challenges to be addressed, even for single-phase flow. As in any method, near-wall behavior may be compromised if sufficient care is not taken in the surface boundary condition scheme. This is particularly important for digital rock, where the surface to volume ratio is large and near-wall flow behavior has a dominant impact on the results. Moreover, in order to simulate a sufficient volume of rock to be representative, the grid resolution must be chosen so as to keep the computational costs manageable. In practice, this means resolving much of the pore space, including critical pore throats, with only a small number of grid cells. Hence for digital rocks there is a high burden on the surface boundary condition scheme to perform adequately under coarse grid conditions.

This paper examines the use of LBM with a surfel-based boundary scheme [10,11] for application to digital rocks. This particular surface treatment has the potential to perform well even for complex geometry and relatively coarse resolution conditions. To demonstrate the efficacy of the present approach, a basic academic case (packed spheres) and a real rock study (perforation damage in Berea sandstone) are presented.

NUMERICAL METHOD

Simulations are carried out using LBM with the wall boundary condition scheme given in [10,11], which employs a set of connected planar facets. These surface elements (“surfels”) provide a high fidelity geometric representation of the boundary and precise control of surface fluxes. To highlight the importance of the boundary scheme for digital rocks, Figure 1 shows a zoom-in of a tiny portion of a 2D slice of a real Berea sandstone image, comparing the stair-step boundary formed by the underlying cubic grid (1a) to the surfel-based boundary (1b), where a realistic (i.e. practical) grid resolution has been chosen. To alleviate stair-step boundaries, other LBM implementations commonly use point-wise interpolation schemes [12,13]; however, these methods face challenges in controlling the fluxes at the wall, such as ensuring exact mass conservation. In contrast, the volumetric-based scheme used here provides precisely defined boundary locations, precise control of surface fluxes, and robust handling of complex geometry.

PACKED SPHERES STUDY

Flow around cubic-centered packed spheres (CCPS), which can be thought of as a simple porous medium, is simulated using the described LBM method. Figure 2 illustrates the configuration of spherical “grains” of diameter D, resulting in an inscribed radius

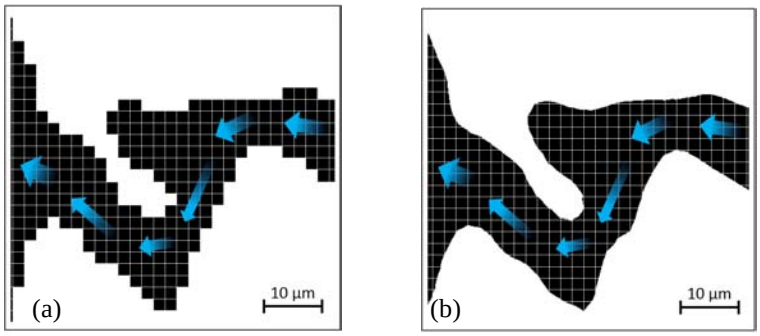

Figure 1: A small portion of a 2D slice of a Berea sandstone digital rock image for use in LBM flow simulation, comparing (a) stair-step surface representation and (b) surfel-based representation.

(effectively the pore radius) $R_t = D(\sqrt{2}-1)/2$. The grains in this simulation are in contact with each other (no gap); hence even this simple case provides a challenging geometry condition at the contact points. The reference solution for absolute permeability k is given by the Kozeny-Carman equation $k = \phi^3 D^3/[72\tau(1-\phi)^2]$ for porosity ϕ, grain diameter D, and tortuosity τ. This particular geometry is known to have $\phi = 0.476$ and $\tau = 2.08$, resulting in absolute permeability $k/D^2 = 0.00262$. The simulation uses a body force to drive the flow and periodic boundaries, with Reynolds number kept well below unity to ensure Darcy flow conditions.

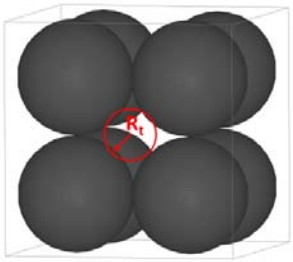

Figure 2: Cubic-centered packed spheres.

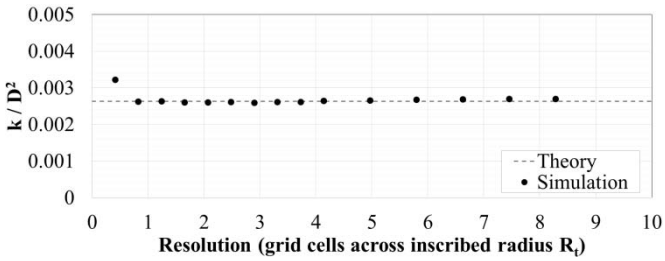

Figure 3: CCPS predicted k vs grid resolution.

Figure 3 plots the simulation results for permeability versus the number of grid cells across R_t. For $R_t \geq 1$ (corresponding to $D \geq 4.8$) the results are in excellent agreement with the reference solution, demonstrating accurate flow behavior even for very coarse grid resolution. Other LBM boundary schemes require higher resolution [14].

PERFORATION DAMAGE STUDY

For well completions in the oil and gas industry, shaped charge jet perforation is the most widely used method of establishing hydraulic communication between the formation and the wellbore [15]. A primary objective of this method is to create tunnels that efficiently transport hydrocarbons. However, detonation of the explosive charge compresses the formation, resulting in a damage zone of compacted rock adjacent to the perforation tunnel which can have significantly reduced permeability. Characterization of the altered

permeability is an important factor in designing perforating jobs, but it is impractical to obtain the desired information from traditional laboratory methods.

In this work, an API RP19B-Section IV test is conducted using a Berea sandstone core. The perforated core is then sectioned and small core plugs drilled from various tunnel sections (Figure 4). For each plug, 3D images are obtained from a micro-CT scanner, and image processing is used to segment the images into grain vs pore regions to provide a geometric representation of the pore-space. Presented here is analysis of one plug (3 mm dia. by 12 mm length) taken from a section near the perforation tunnel opening. The entire plug is imaged by a series of 4 scans at resolution 2.4 μm, with the scans partly overlapping to enable a continuous reconstruction (Figure 5). The domain is subdivided into 6 regions for analysis. Pore size distributions are determined using a maximum sphere method [16], and flow simulations using the present LBM approach [10,11] are performed for absolute permeability prediction. A one-to-one mapping of grid cells to scan voxels was chosen for the LBM flow simulations.

Figure 4: (a) Perforated core cut into sections; (b) section of tunnel with 3x12mm plug (c) drilled out.

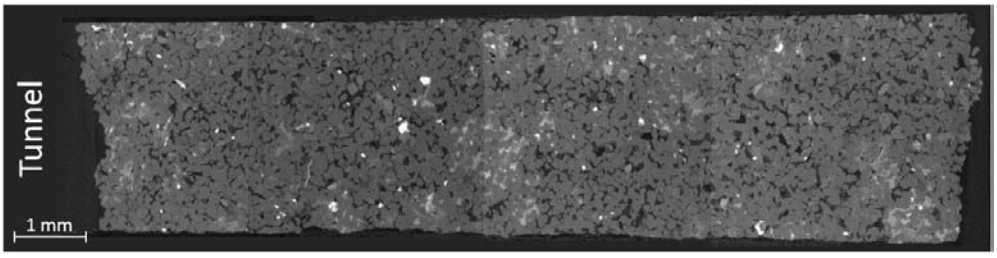

Figure 5: Center-plane of reconstructed micro-CT images of test section plug.

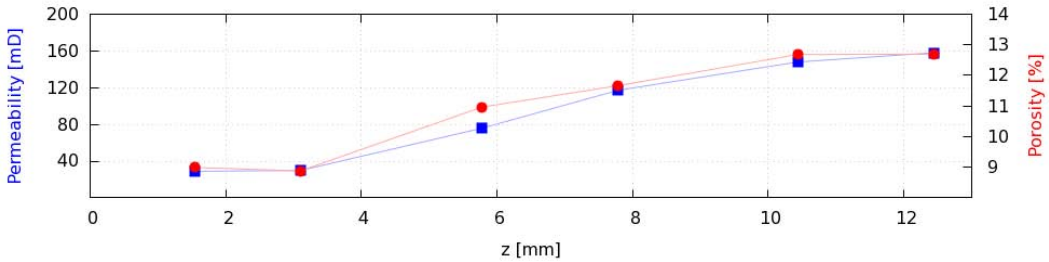

Figure 6: Porosity (right y-axis) and absolute permeability (left y-axis) of test section plug.

Figure 6 shows the resulting porosity and absolute permeability profiles through the plug, aligned to match Figure 5; the x-axis indicates distance from the tunnel surface (i.e. going

deeper into the rock). It is seen that the damage zone extends ~10 mm for this tunnel location, and the permeability variation is well correlated with the porosity. In the transition from damaged to native regime, porosity changes from 9% to 12% (~25% variation), whereas permeability changes from 30 mD to 160 mD (~530% variation).

To highlight the shaped charge explosion impact on pore structure, a 2D plane from the damage zone is compared to one from the native rock region in Figure 7, where the pore space is colored by local pore size (min. blue, max. red). Fewer large pores and more small pores are seen in the damaged rock. Pore size distributions for native and damaged rock are quantitatively compared in Figure 8, which plots volume fraction of pore space occupied by pores of radius R versus R; the shift to smaller pores in the damage zone is readily seen. Note that a significant volume fraction is associated with small pores, with the most frequent pore radius having 2-3 grid cells; this highlights the importance of achieving accurate simulated flow behavior for such coarse resolution conditions.

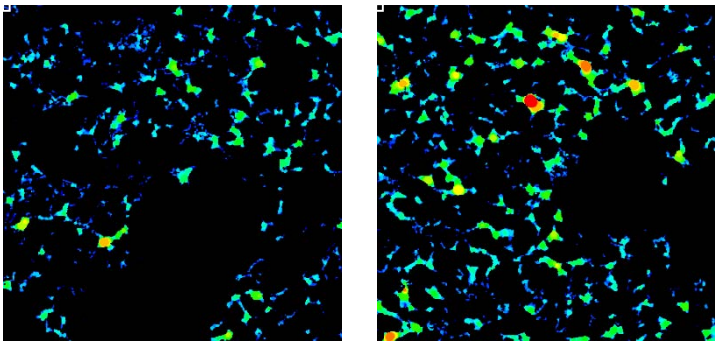

Figure 7: Pore space colored by local pore size for damaged rock (left) and native rock (right).

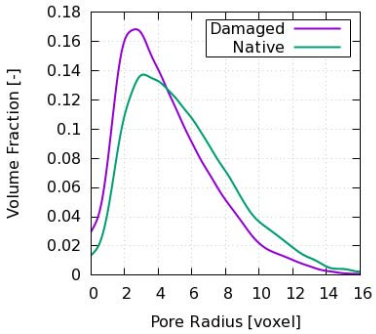

Figure 8: Pore size distributions.

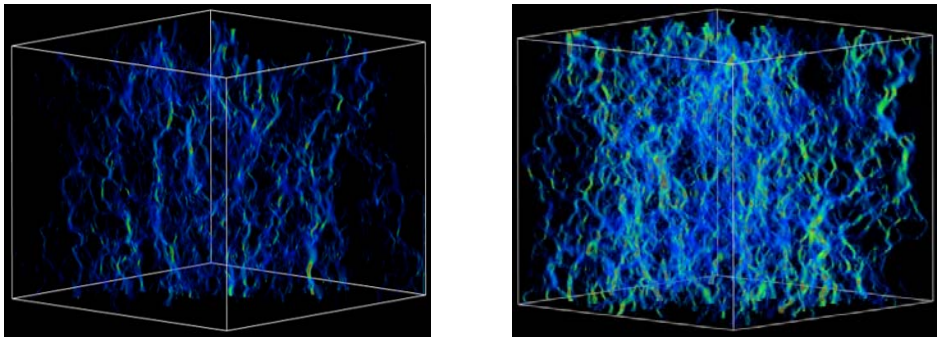

Figure 9: Visualization of local velocity field in damaged rock region (left) and native rock region (right).

In Figure 9, the local velocity field is visualized for damaged rock compared to native rock, using opacity to emphasize the high velocity locations. The overall flow in the damaged rock appears lower, with fewer connected paths involved in contributing significantly to the flow conduction.

CONCLUSION

A lattice-Boltzmann based method incorporating the surfel-based boundary technique is examined for application to digital rock pore-scale flow simulation. A grid resolution study of flow past cubic centered packed spheres demonstrates accurate prediction of single-phase absolute permeability with resolution as low as one grid cell across the inscribed (effective pore) radius. The ability to remain accurate at such coarse resolution is highly advantageous for minimizing the computational cost of digital rock cases where it is important to have a large enough field of view to simulate a statistically representative region of pore space. Application to a real digital rock study characterizing the damage zone around a perforation tunnel is demonstrated using a micro-CT image of a sample plug from the tunnel. Profiles of porosity and absolute permeability through the damage zone out to native rock are determined. Visualization of pore size distribution and flow within the pore space of the rock are presented and highlight the observed trends. Most of the pore space is resolved with a small number of grid cells per effective pore radius, with the pore size distribution peaking at about 3 grid cells; therefore, the demonstrated accuracy of the numerical scheme at such coarse resolution is of critical importance to the reliability of the real rock simulation results.

REFERENCES

1. S. Chen, G. Doolen, “Lattice Boltzmann method for fluid flows”, Annu. Rev. Fluid Mech. 30:329 (1998)
2. S. Chen, H. Chen et al, “Lattice Boltzmann model for simulation of magnetohydrodynamics”, Phys. Rev. Lett. 67, 3776 (1991)
3. H. Chen, S. Chen, W. Matthaeus, “Recovery of the Navier-Stokes equations using a lattice-gas Boltzmann method”, Phys. Rev. A 45, 5339 (1992)
4. Y. Qian, D. d'Humieres, P. Lallemand, “Lattice BGK models for Navier-Stokes equation”, Europhys.Lett 17, 479 (1992)
5. H. Chen, C. Teixeira, K. Molvig, “Digital physics approach to computational fluid dynamics: some basic theoretical features”, Intl. J. Mod. Phys. C 9, No.8, 1281 (1998)
6. H. Chen, S. Kandasamy et al, “Extended-Boltzmann Kinetic Equation for Turbulent Flows”, Science, Vol 301, Issue 5633, 633 (2003)
7. H. Andra, N. Combaret et al, “Digital rock physics benchmarks – part II: Computing effective properties”, Comp. Geosci. 50, 33 (2013)
8. H. Andra, N. Combaret et al, “Digital rock physics benchmarks – part I: Imaging and segmentation”, Comp. Geosci. 50, 33 (2013)
9. X. Shan, H. Chen, “Lattice Boltzmann model for simulating flows with multiple phases and components”, Phys Rev E 47, 1815 (1993)
10. H. Chen, C. Teixeira, K. Molvig, “Realization of Fluid Boundary Conditions via Discrete Boltzmann Dynamics”, Int. J. Mod. Phys. C 09, 1281 (1998)
11. H. Chen, “Volumetric formulation of the lattice Boltzmann method for fluid dynamics: Basic concept”, Phys. Rev. E 58:033955 (1998)
12. X. He, and G. Doolen, “Lattice Boltzmann method on curvilinear coordinates system: vortex shedding behind a circular cylinder”, Phys. Rev. E 56, 434 (1997).
13. I. Ginzburg, D. d'Humieres, “Multireflection boundary conditions for lattice Boltzmann models”, Phys. Rev. E 68:066614 (2003)
14. C .Pan, L. Luo, C. Miller “An evaluation of lattice Boltzmann schemes for porous medium flow simulation”, Comp. & Fluids 35, 898 (2006)
15. N. Osarumwense, R. Satti et al, “Shaped Charge Selection and Underbalance Optimization Using the Perforation Flow Laboratory for Deepwater Subsea Wells in Offshore Africa”, 2014 SPE Deepwater Drilling & Completions Conf, SPE-170259-MS.
16. H. Dong and M. Blunt, "Pore-network extraction from micro-computerized-tomography images", Phys. Rev. E 80:036307 (2009)